Earthquake Engineering, Tenth World Conference © 1992 Balkema, Rotterdam. ISBN 90 5410 060 5

Dynamic behavior of pile group in liquefied sand deposit

Yuji Miyamoto, Yuji Sako & Kenji Miura
Kajima Corporation, Japan

Ronald F. Scott & Behnam Hushmand
California Institute of Technology, Calif., USA

ABSTRACT: Dynamic centrifuge tests were performed to develop an understanding of soil-pile foundation interaction and to provide data for verification of an earthquake response analysis method for pile foundations in liquefiable soil during earthquakes. Centrifugal test results indicate that pile foundation response in nonlinear liquefied sand is greatly affected by soil behavior due to large ground displacement and excess pore water pressure buildup. The numerical model which consists of beam elements and nonlinear lateral Winkler springs, taking into account the changing effective stress, is discussed by comparing predicted results with measured results.

1 INTRODUCTION

Behavior of a structure built on pile foundation is greatly affected by nonlinear soil-pile foundation interaction during strong earthquakes. Particularly in liquefiable sand deposit, further complicated interaction between piles and the surrounding saturated soil will occur because of pore water pressure generation and large displacement. An improved aseismic design method is then required to take into account nonlinear soil-pile foundation interaction on earthquake response. However, very few experimental studies have investigated pile foundation responses in liquefiable sand deposits during strong earthquakes. The earthquake response of a pile foundation in liquefiable soil during strong earthquakes is usually studied using a two-dimensional finite element method or a beam-Winkler spring model, incorporating effective stress analysis models. These analysis methods also lack confirmation.

The object of this study is to develop an understanding of soil-pile foundation interaction effects in a liquefiable soil deposit. Dynamic centrifugal tests were performed under a centrifugal acceleration of 50g on a model consisting of a rigid pile cap and a four-pile group embedded in saturated fine sand. Correlation analyses were also conducted on the test results using a practical simplified computer code incorporating an effective stress method.

2 CENTRIFUGAL MODEL TEST

2.1 *Centrifuge equipment and test model*

The centrifuge employed at the California Institute of Technology has an approximate effective radius of 1m, and a maximum acceleration of about 175g. It is equipped with a one-degree-of-freedom shaking table and data acquisition system. The soil container(laminar box) is a rectangular box made of 1.27cm-thick aluminum layers separated by placing roller bearings between them to reduce boundary effects(Hushmand and Scott(1988)). The soil container, measured internally, is 35.6cm long x 17.8cm wide x 25.4cm depth. Dynamic centrifugal tests on a pile foundation model were performed at 50g. Scaling relations in a centrifugal model are shown in Table 1. Thus, if the soil model is made of the same material as the prototype, the stresses in the model are the same as in the prototype. Soil property in centrifugal test represents that of the prototype. In these tests, deaired water was employed because the grain size of the sand used was smaller than that of the prototype and the effect of the density and the viscosity of pore fluid on the test results is still not clear. According to the similarity rule, excess pore water pressure dissipation occurs 50 times faster than it would in the equivalent prototype with the same soil.

Fig.1 shows the test model and the positions of measuring instruments. The dimensions in this figure indicate the mean values measured after each test condition in the prototype scale. The pile foundation model consisted of a rigid pile cap and a four-pile group. The piles were rigidly attached to the pile cap, the weight of which was 85.2 ton in the prototype. The model piles represented prototype tubular-steel piles of diameter 0.48m, wall thickness 13mm and length 10.7m, with pile spacings of 2.5 diameters. The bending stiffness of the pile was 10.9×10^3 t/m^2 in the prototype scale. The soil used in the tests was Nevada sand #120 of 0.1mm mean grain size. The physical properties of this sand are listed in Table 2. The 1g total unit weight of the saturated sand, after consolidation at 50g, was 1.98 t/m^3 and its relative density was 43%.

2.2 *Instrumentation and test procedures*

The instruments employed in the tests, as shown in Fig.1, were 4 accelerometers(AH), 3 linear variable

Table 1. Similarity rule in centrifugal model test

Quantity	Full Scale (prototype)	Centrifuge Model at n g's
Linear Dimension	1	1/n
Volume	1	$1/n^3$
Time :		
Dynamic Events	1	1/n
Hydrodynamic Events	1	$1/n^2$
Velocity	1	1
Acceleration	1	n
Mass	1	$1/n^3$
Stress	1	1
Strain	1	1
Density	1	1
Frequency	1	n

Table 2. Physical properties of Nevada sand #120

Specific gravity	G_s	2.66
Max. void ratio	$e_{max.}$	0.83
Min. void ratio	$e_{min.}$	0.51
Uniformity coeff.	U_c	1.95
Mean grain size	D_{50}	0.1 (mm)

differential transducers(LT), 4 strain gauges(SG) for measuring pile bending moments and 4 pore water pressure transducers(PP). The input acceleration had a spectrum similar to that of the 1940 El Centro earthquake strong motion record NS component. The maximum input accelerations measured at the soil container base(AH1) were about 100gal(TEST-S1) and 250gal(TEST-S2). In these tests, the centrifuge was gradually brought up to 50g and a steady acceleration of 50g was maintained for 20 minutes before earthquake excitation to saturate the soil completely.

2.3 *Test results*

The test results shown below are adjusted for the prototype scale. Fig.2 shows typical acceleration time histories with the input motion, pile bending moments, excess pore water pressures and ground relative displacement measured in TEST-S1 and TEST-S2.

It is observed that the acceleration(AH3) at GL-0.75m in the ground for the high level input(TEST-S2) are amplified in the lower frequency content compared with that in the low level input(TEST-S1). The acceleration(AH4) at the pile cap is filtered in the high frequency range. The horizontal relative displacement (LT3) at GL-0.75m in TEST-S2 is much larger than that in TEST-S1. The amplifications in the sand layer of the maximum accelerations in the base input cannot be seen in TEST-S2, and amplification ratio at the pile cap is smaller than that in TEST-S1.

The excess pore water pressures are generated at the beginning of the base input, and subsequently decay according to the intensity of the input acceleration. It seems probable that the high-frequency fluctuations observed in the pore water pressure time histories are

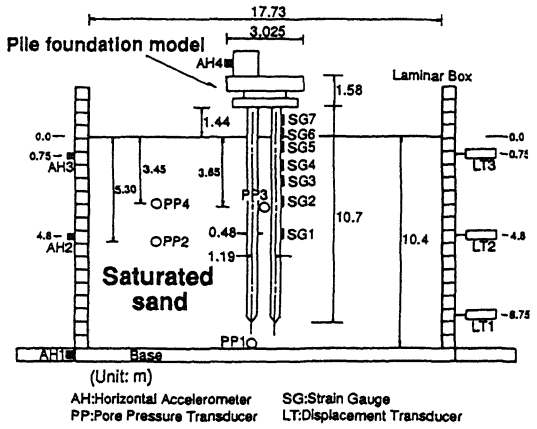

Fig.1 Centrifugal model indicated in prototype scale

due to compression waves generated in the saturated sand by the vertical vibration of the soil container. The ratio of the peak excess pore water pressure to the initial effective stress is about 1.0 at GL-3.45m(PP4) and about 0.68 at GL-5.30m(PP2) in TEST-S2, so that the upper layer of sand almost reached complete soil liquefaction. This peak excess pore water pressure at PP4 occurred at about 13 seconds, at which a large amplitude with low frequency can be seen in the pile cap acceleration, pile bending moments and ground displacement time histories thereafter. The pile bending moment time histories are similar to that of the pile cap which result from the ground responses. Large bending moments are generated in the middle of the ground. This is more obvious in the result of TEST-S2, in which large ground displacement occurs due to soil liquefaction.

The acceleration response spectra for 5 per cent damping for GL-4.8m, GL-0.75m in the ground and the pile cap are shown in Fig.3. The predominant frequency of the soil-pile foundation system can be seen at about 2.3 Hz in TEST-S1 and this shifts to about 1.0 Hz in TEST-S2.

3 CORRELATION ANALYSES

3.1 *Analysis method*

Correlation analyses for the centrifugal test results were conducted using a beam-Winkler spring model, as shown in Fig.4. In this analysis procedure, the nonlinear effective stress method, computer program DESRA proposed by Finn(1977) was utilized for the free ground response. The obtained free ground responses, including displacement and excess pore water pressures, were applied to the soil-pile foundation system as earthquake input. Superstructure and pile foundation were idealized by a one-stick model with lumped masses and bending-shear elements. The lumped masses were connected to free ground through nonlinear Winkler springs modified at each step in accordance with the generation and dissipation of excess pore water pressures. The linear rotational spring, related to the axial stiffness of the piles, was also incorporated at the pile head.

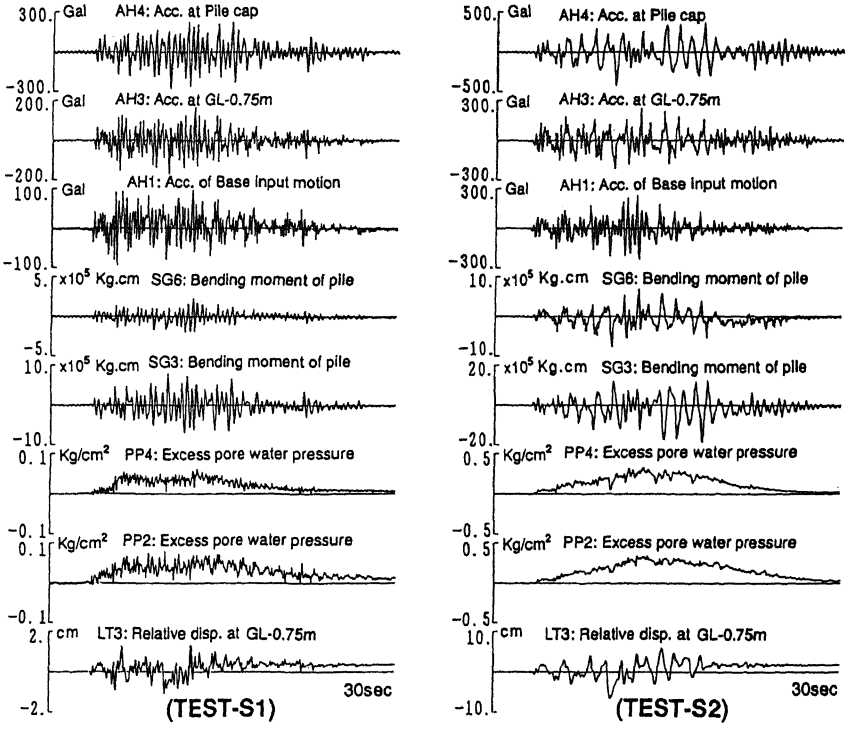

Fig.2 Measured time histories in TEST-S1, TEST-S2

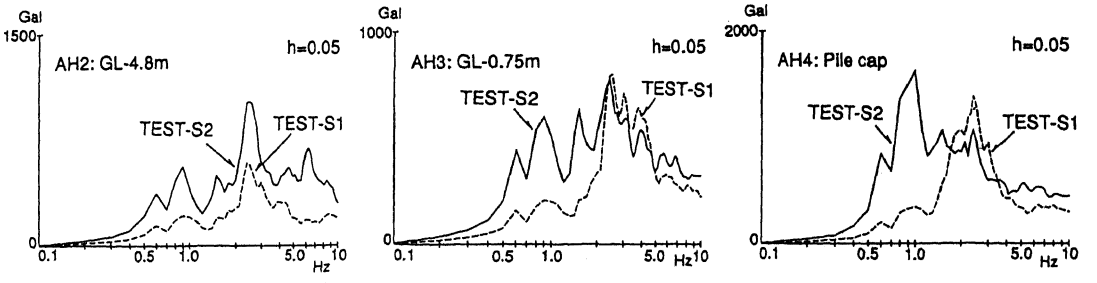

Fig.3 Comparisons of acceleration response spectra in TEST-S1, TEST-S2

The computer program DESRA is based on the shear stress-strain relationship of the Hardin-Drnevich model with the Masing rule expressed as

$$\tau = G_0 \gamma / (1+G_0 \gamma / \tau_{max}) \quad (1)$$

in which τ = shear stress, τ_{max} = shear strength, γ = shear strain and G_0 = initial shear modulus. The initial shear modulus G_0 and shear strength τ_{max} are modified progressively for the changing vertical effective stress of saturated sand subjected to an earthquake. Physical constants employed in correlation analyses for the saturated sand are indicated in Table 3. The initial shear modulus G_0 employed in the Hardin-Drnevich model is estimated from

$$G_0 = A \{(2.17 - e)^2 / (1 + e)\} (\sigma'_{m0})^{1/2} \quad (2)$$

in which e = void ratio and σ'_{m0} = initial mean effective stress. The coefficient A, obtained from the resonant-column tests, is modified to correspond with the resonance frequency of the free ground in TEST-S1. The shear strength τ_{max} is obtained by the Mohr-Coulomb yield condition.

The pore water pressure generation Δu is defined by

$$\Delta u = E_r \Delta \varepsilon_{vd} \quad (3)$$

where

$$\Delta \varepsilon_{vd} = C_1(\gamma - C_2 \varepsilon_{vd}) + C_3 \varepsilon^2_{vd} / (\gamma + C_4 \varepsilon_{vd}) \quad (4)$$

$$E_r = (\sigma')^{1-m} / m K_2 (\sigma'_0)^{n-m} \quad (5)$$

in which E_r = one-dimensional rebound modulus of sand at an effective stress σ', $\Delta \varepsilon_{vd}$ = volumetric strain increment under simple shear condition. Parameters C_1, C_2, C_3 and C_4 ,and K_2, m and n are estimated according to the cyclic simple shear tests and one-dimensional loading and unloading tests. These

Table 3. Physical soil constants for analyses

Soil : Nevada sand #120	
Internal friction angle: ϕ'	35°
Void ratio: e	0.69
Density: γ_t	1.98 t/m^3
Permeability: k	5.2x10^{-3} cm/sec
Coef. of earth pressure at rest: K_0	0.45
Shear modulus: G_0	570(GL-0.6m) - 3330(GL-10.4m)t/m^2

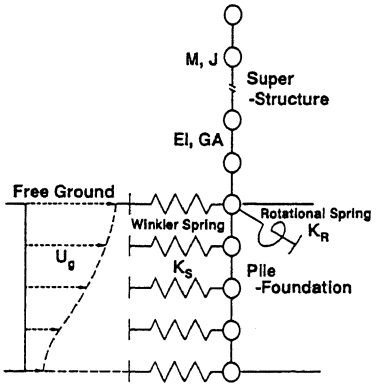

Fig.4 Numerical model for soil-pile foundation system

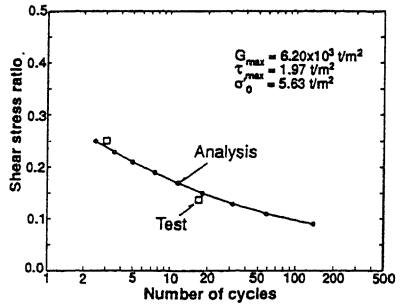

Fig.5 Liquefaction resistance curve by analysis and cyclic simple shear tests.

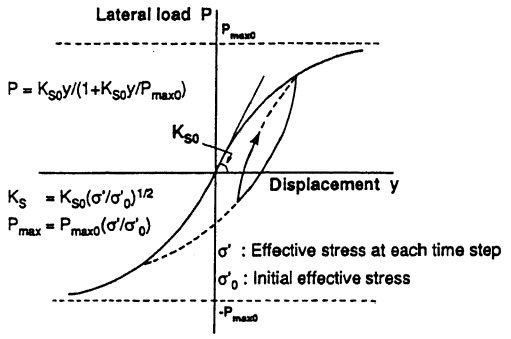

Fig.6 Nonlinear lateral load-displacement relationship of Winkler spring

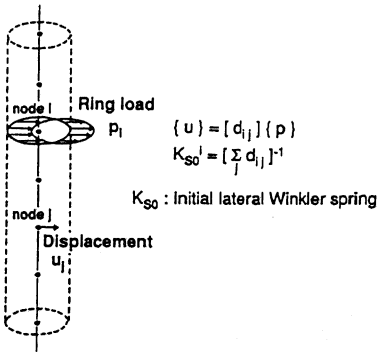

Fig.7 Evaluation of initial lateral Winkler spring by ring load in a layered stratum

parameters are also modified to simulate liquefaction resistances obtained from the cyclic simple shear test results. The values employed in the correlation analyses are C_1=0.114, C_2=1.2, C_3=0.17 and C_4=1.36, and K_2=0.001(t/m^2), m=0.1 and n=0.19. Fig.5 indicates the liquefaction resistance curve calculated using these parameters in comparison with the cyclic simple shear test results of undrained saturated sand.

The nonlinear lateral load-displacement relationship of a pile is also based on the Hardin-Drnevich model with the Masing rule as shown in Fig. 6. Initial lateral Winkler springs K_{s0} at each depth are evaluated by the inversion of soil flexibilities by ring loads at the nodes as shown in Fig. 7. The position of the node corresponds to that of the local lumped mass of the pile. The soil displacements can be expressed as

$$\{u\} = [\, d_{ij} \,]\{p\} \qquad (6)$$

where {u} and {p} are the vectors of lateral displacement and load at the nodes, [d_{ij}] is the flexibility matrix of the soil. The soil displacements {u} caused by lateral ring loads {p} in a layered stratum (Kausel(1982)) are calculated at low frequency (f=0.25Hz) to form the flexibility matrix. The soil flexibility at the i-th node is approximately obtained from the superposition of soil displacements at the i-th node caused by ring loads at all nodes. Then, the lateral Winkler spring at the i-th node is obtained from the inversion of the soil flexibility expressed as

$$K_{s0}^i = [\, \Sigma_j \, d_{ij} \,]^{-1} \qquad (7)$$

where K_{s0}^i is the initial lateral Winkler spring at the i-th node. Shear modulus values for evaluating initial lateral Winkler springs are estimated by the secant modulus of the backbone curve of each layer at the effective shear strain($0.65\gamma_{max}$), which is obtained from the nonlinear free ground response. The initial ultimate lateral soil resistance P_{max0}^i at the i-th node is assumed by Broms(1965) to be three times the Rankine passive pressure expressed as

$$P_{max0}^i = 3\,\sigma'_0\,K_p\,d\,l \qquad (8)$$

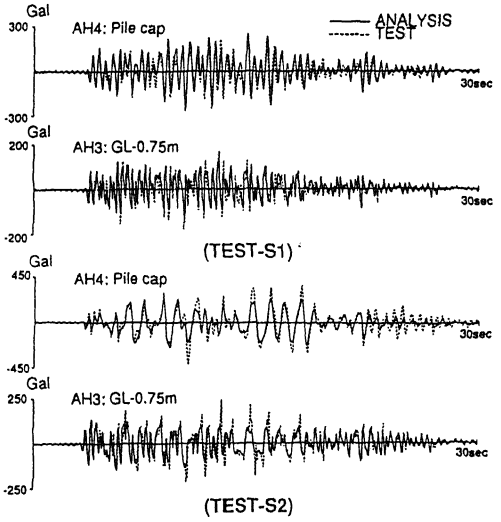

Fig.8 Comparisons of predicted accelerations with TEST-S1 and TEST-S2

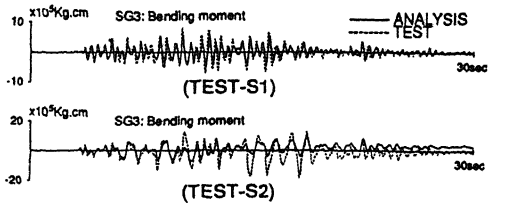

Fig.9 Comparisons of predicted pile bending moments with TEST-S1 and TEST-S2

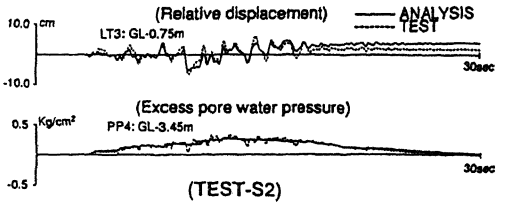

Fig.10 Comparisons of predicted ground relative displacement and excess pore water pressure with TEST-S2

where σ'_0 is the initial effective stress, $K_p = (1+\sin\phi')/(1-\sin\phi')$, ϕ' is the internal friction angle, d is pile diameter and l is pile length equivalent to the i-th node.

The pile group effect for initial lateral Winkler spring and ultimate lateral soil resistance is taken into account using the pile group efficiency α_H defined by

$$\alpha_H = K_H^N / (N K_H^S) \quad (9)$$

where N, K_H^N and K_H^S are the number of piles, the value of horizontal static impedance at pile head of N-piles and its value for a single pile respectively. The value of α_H is obtained as 0.56 by the three-dimensional thin layered element method (Masuda(1987)) using the degraded shear modulus of soil. The equivalent lateral Winkler spring K_{s0}^e and the ultimate lateral soil resistance P_{max0}^e taking account of the pile group effect are approximately defined by

$$K_{s0}^e = \alpha_H N K_{s0} \quad (10)$$

$$P_{max0}^e = \alpha_H N P_{max0} \quad (11)$$

where $\alpha_H N$ is the equivalent number of piles. The values of K_s and P_{max} at each time step in the time domain are also modified according to the change of the effective stress defined by

$$K_s = K_{s0}^e (\sigma' / \sigma'_0)^{1/2} \quad (12)$$

$$P_{max} = P_{max0}^e (\sigma' / \sigma'_0) \quad (13)$$

where σ' is the effective stress at each time step and σ'_0 is the initial effective stress.

The rotational spring under a pinned condition at the pile head is also evaluated by the three-dimensional thin layered element method using the degraded shear modulus of soil.

The viscous damping employed are 1 per cent for pile foundation, 5 per cent for the lateral springs and 30 per cent for the rotational spring at the first natural frequency by the eigenvalue analysis.

3.2 *Results of analysis*

Fig.8 indicates the predicted acceleration time histories at GL-0.75m and the pile cap as compared with TEST-S1, S2. Fig.9 also indicates comparisons of bending moments at SG3. Fig.10 indicates comparisons of ground relative displacement and excess pore water pressure in TEST-S2. Acceleration response spectra for 5 per cent damping are indicated in Fig.11.

In TEST-S1, the acceleration response spectrum at GL-4.8m is smaller than the measured result. The predicted responses at GL-0.75m and the pile cap, however, show good agreement with the measured results.

In TEST-S2, the predicted responses, except for the peak amplitudes, also agree well with the measured results, including the relative ground displacement and the processes of excess pore water pressures. It is found that the shift in the predominant frequency of the soil-pile foundation system by soil liquefaction is represented well by the proposed model. The predicted pile bending moment in TEST-S1 corresponds to the measured results, but the peak amplitudes in TEST-S2 are underestimated. The underestimated peak amplitudes in accelerations and bending moment by analysis in TEST-S2 are mainly attributed to the discrepancies in the free ground response. It is considered that these discrepancies are due to the dilatancy of soil during large strain.

Fig.12 indicates the calculated lateral load-displacement relationships of the pile at GL-0.6m and GL-3.0m for TEST-S2. It can be seen that the value of lateral springs are degraded by the increase of pile displacement and the decrease of effective stress. The degradations at GL-0.6m are much larger than at GL-

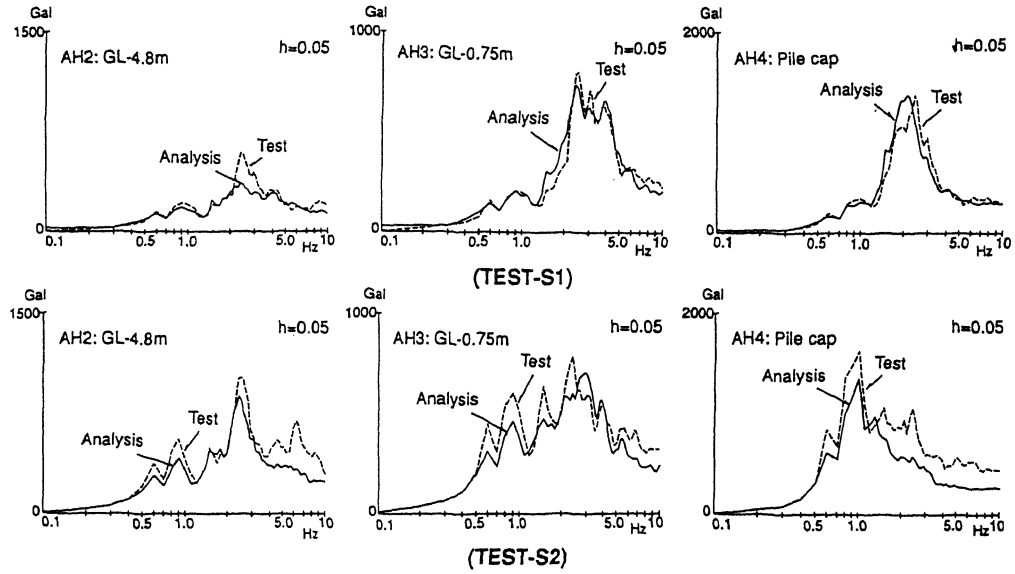

Fig.11 Comparisons of predicted acceleration response spectra with TEST-S1, S2

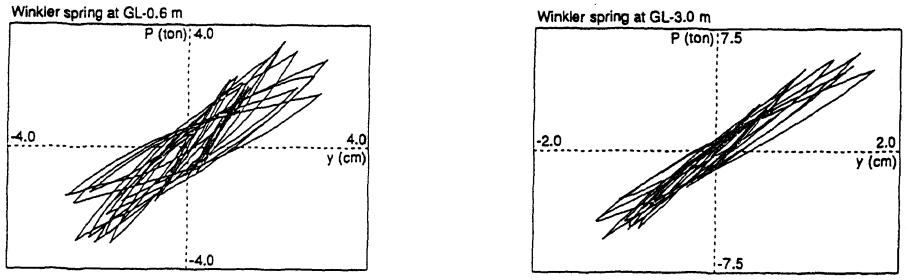

Fig.12 Calculated lateral load-displacement relationships in TEST-S2 analysis

3.0m due to large displacement and excess pore water pressure buildup near the ground surface.

4 CONCLUSIONS

Centrifugal test results indicate that pile foundation response in liquefied soil, including maximum bending moment, change remarkably due to large ground displacement and excess pore water pressure buildup.

The proposed numerical model can effectively predict pile foundation response in liquefied soil. The numerical model, however, indicates somewhat underestimated responses and is based on some assumptions in modeling the soil-pile foundation system. Further studies should be performed to advance the evaluation of pile foundation response in nonlinear liquefiable soil during strong earthquakes.

ACKNOWLEDGMENT

The research described was conducted as one of the topics in the KAJIMA-CUREe (California Universities for Research in Earthquake Engineering) Project. The authors wish to express their appreciation to Dr. T. Kobori, Professor Emeritus of Kyoto University, for his insightful suggestions and discussions, and also Mr. K. Masuda, Mr. S. Uchiyama, Mr. K. Suzuki, Mr. E. Kitamura and Mr. M. Nagano, Kajima Corporation, for their cooperation.

REFERENCES

Broms, B.B. 1965. Design of laterally loaded piles: *Journal of the Soil Mechanics and Foundations Division.* ASCE. Vol.91: 79-99.

Finn, W.D.L., et al. 1977. An effective stress model for liquefaction: *Journal of the Geotechnical Eng. Division.* ASCE. Vol.103: 517-533.

Hushmand, B., et al. 1988. Centrifuge liquefaction tests in a laminar box: *Geotechnique.* Vol.38: 253-262.

Kausel, E., et al. 1982. Dynamic loads in the interior of a layered stratum- An explicit solution-: *Bulletin of the Seismological Society of America.* Vol.72: 1459-1481

Masuda, K., et al. 1987. Simulation analysis of forced vibration test for actual pile foundation by thin layer method. *Proc. of Reliability and Robustness of Eng. Software Conf.*